Single molecule localization microscopy of the distribution of chromatin using Hoechst and DAPI fluorescent probes

Aleksander T Szczurek[1,†], Kirti Prakash[1,2,†], Hyun-Keun Lee[1,3,†], Dominika J Żurek-Biesiada[4], Gerrit Best[5,6], Martin Hagmann[5,6], Jurek W Dobrucki[4], Christoph Cremer[1,2,3,5], and Udo Birk[1,3,5,*]

[1]Institute of Molecular Biology; Mainz, Germany; [2]Institute for Pharmacy and Molecular Biotechnology; University of Heidelberg; Heidelberg, Germany; [3]Department of Physics; University of Mainz; Mainz, Germany; [4]Faculty of Biochemistry, Biophysics, and Biotechnology; Jagiellonian University; Kraków, Poland; [5]Kirchhoff Institute for Physics; University of Heidelberg; Heidelberg, Germany; [6]University Hospital Heidelberg; University of Heidelberg; Heidelberg, Germany

[†]These authors contributed equally to this work.

Several approaches have been described to fluorescently label and image DNA and chromatin in situ on the single-molecule level. These superresolution microscopy techniques are based on detecting optically isolated, fluorescently tagged anti-histone antibodies, fluorescently labeled DNA precursor analogs, or fluorescent dyes bound to DNA. Presently they suffer from various drawbacks such as low labeling efficiency or interference with DNA structure. In this report, we demonstrate that DNA minor groove binding dyes, such as Hoechst 33258, Hoechst 33342, and DAPI, can be effectively employed in single molecule localization microscopy (SMLM) with high optical and structural resolution. Upon illumination with low intensity 405 nm light, a small subpopulation of these molecules stochastically undergoes photoconversion from the original blue-emitting form to a green-emitting form. Using a 491 nm laser excitation, fluorescence of these green-emitting, optically isolated molecules was registered until "bleached". This procedure facilitated substantially the optical isolation and localization of large numbers of individual dye molecules bound to DNA in situ, in nuclei of fixed mammalian cells, or in mitotic chromosomes, and enabled the reconstruction of high-quality DNA density maps. We anticipate that this approach will provide new insights into DNA replication, DNA repair, gene transcription, and other nuclear processes.

Introduction

In order to study the functional architecture of chromatin at the nanoscale, highest resolution light microscopy of DNA in intact 3D cell nuclei should prove to be a major source of information. Several attempts to investigate chromatin nanostructure by super-resolution microscopy have been undertaken either by detecting the GFP-tagged core histones,[1-3] or by imaging fluorescently labeled DNA, using cyanine intercalators[4,5] (YOYO-1, TO-PRO-1), minor groove binders[4,5] (SYTO, PicoGreen), or by a special bleaching-based approach termed generalized single molecule high-resolution imaging with photobleaching (gSHRImP) on POPO-3 labeled DNA.[6] DNA intercalators, however, can interfere with the DNA structure.[24] Recently, super-resolution on the single molecule detection level using a DNA precursor analog, 5-ethynyl-2′-deoxyuridine (EdU), was reported, following incubation throughout a complete cell cycle.[7] EdU was labeled with a standard fluorophore using a "click" reaction. However, such long-term incorporation of DNA precursor analogs results in toxicity[8] (affecting cells before fixation) and in a variety of staining patterns.

So far, all methods for direct single molecule localization microscopy of nuclear DNA have suffered from serious drawbacks. The lack of a proper tool for accurate direct imaging of DNA nanostructures poses a major obstacle to the investigation of nuclear processes such as studies of spatial relationships between global DNA distribution and specific replication units, transcription and splicing complexes, or linker DNA and nucleosome core proteins (for a review see[9]). The recently described UV-induced photoconversion of standard DNA

minor groove binding dyes opens new opportunities in super-resolution imaging of chromatin in situ. In combination with the aforementioned questions related to nuclear nanostructures, this UV-induced photoconversion of DNA minor groove binding dyes promotes super-resolution imaging of chromatin in situ.[10,11]

Among a wide variety of DNA stains applied in fluorescence microscopy, the DNA minor groove binders bisbenzimide Hoechst and DAPI are the two most commonly used. Both have their excitation maxima around 360 nm and their emission maxima around 460 nm. Recently it has been shown that both dyes can be readily converted from the blue-emitting state to their green-emitting derivatives upon illumination with UV[10,11] or 405 nm laser light.[11] Mass spectrometry studies demonstrated that under these circumstances Hoechst 33258 and DAPI undergo protonation.[11] Interestingly, conversion of the blue-emitting into the green-emitting forms of these dyes may be driven by hydrogen peroxide as well.[11] When excited with a 458 nm Ar+ laser line, these photoconverted forms of Hoechst 33258 and DAPI emit green fluorescence, with the emission maxima shifted from 465 nm to 530 nm (Hoechst) and from 454 nm to 505 nm (DAPI).[11] Furthermore, the photoconverted green-emitting forms of the dyes are bleached readily under blue excitation.[11]

Here we took advantage of these exceptional features of Hoechst and DAPI dyes, and employed them in single molecule localization microscopy (SMLM)[12] of DNA in situ. A special SMLM approach, Spectral Position Determination Microscopy (SPDM) with physically modified fluorochromes,[12,13] was applied. In this SMLM variant, blinking of standard fluorophores is induced by appropriate high illumination intensities at suitable excitation wavelengths, in the presence of a chemical environment favoring the processes of both blinking and photoconversion. In this blinking-based imaging approach molecules emit fluorescent bursts[3] after stochastic recovery from a "non-emitting" form until they are bleached. Because of the possibility of multiple bursts being emitted from a single fluorophore, we use the term "signals" rather than "molecules" throughout the text. Means to eliminate such multiple detections in our experiment are described in Materials and Methods.

Interestingly, upon illumination with a high intensity 491 nm laser light, the green-emitting forms of Hoechst- or DAPI-stained DNA exhibit such stochastic blinking, which can be detected in the green-yellow channel. Thus, in a given field of view and at a given moment (under suitable illumination and environmental conditions), only a few, optically isolated molecules reside in the green-emitting fluorescent state. The emission induced by the 491 nm excitation light can be recorded until the molecules are bleached. The center of an individual fluorescent burst designates the position of a single fluorescing molecule in the object space.[12] Subsequently, other molecules stochastically undergo the transition from the blue-emitting to the green-emitting form under simultaneous illumination with 405 nm light, again to be recorded individually. This enables the optical isolation of a number of closely spaced single molecules, and assignment to a joint localization map.

Here, we report on the first successful "nanoimaging" of the positions of Hoechst and DAPI molecules, using localization microscopy of chromatin in fixed mammalian cells, with an average precision of localization of 15–25 nm. Consequently, this new approach allowed us to perform optical imaging of the local distribution of DNA in the cell nucleus and in mitotic chromosomes with a high optical and structural resolution, down to a few tens of nanometers.

Results

Under the conditions used, we could not obtain blinking-based superresolution images from the standard blue-emitting forms of the dyes. In a previous paper we noted that the signals of the green-emitting forms of both dyes, Hoechst 33258 and DAPI, are rather weak under standard experimental conditions.[11] Under these conditions the vast majority of the molecules bound to DNA remains in their blue-emitting form, except for a small fraction of the green-emitting form, which presumably remains in equilibrium with the parent form of the dye.[11] The population of molecules in this green-emitting form can be enriched by 405 nm-induced photoconversion.[11] Controlling the power of the 405 nm illumination, the number of molecules in the green-emitting form can be adjusted to fulfil the criterion of optical isolation required for localization based superresolution.

For detection of the green-emitting molecules, we used 491 nm illumination with appropriate intensities. Without 405 nm illumination, a lower blinking rate in the green-yellow emission channel was observed (see **Fig. S1**) (approximately 11 signals per frame corresponding to 0.08 signals per μm^2). Nonetheless, after the registration of 10 000 frames, the total number of approximately 110 000 detected fluorescent bursts was already sufficient to reconstruct an image based on molecule position information (see example in **Fig. S1**). Then, the 405 nm excitation was switched on, and in the following 10 000 frames, a substantially higher number of optically isolated fluorescence signals was recorded in the same sample region. Hence, at a given number of frames registered, the structural resolution was further enhanced due to a higher number of detected molecules. Subsequently, the 405 nm laser line was used in all further experiments resulting in a continuous replenishment of the population of the green-emitting photoproducts during the measurement.[11] The different illumination modes using two lasers at 405 nm and 491 nm are compared in **Figure 1**. The emission spectra of the original (blue) and the photoconverted (green) forms of Hoechst or DAPI overlap significantly (**Fig. 2G**; **Fig. S2**). We selected a detection band in the green-yellow range (585–675 nm) to minimize crosstalk from the long-wavelength emission tail of the blue-emitting form.

Furthermore, our imaging protocol allows for significantly extended measurement times. The main reason for this is the fact that 491 nm light is only marginally absorbed by the original (blue) forms of the dyes (absorption maxima: Hoechst; λ_{exc} = 355 nm, DAPI; λ_{exc} = 364 nm). After the localization measurement including 405 nm illumination, the fluorescence intensity of the Hoechst 33258 blue-emitting form dropped to 89 ± 4% normalized to 100% prior to the experiment, while in the case without
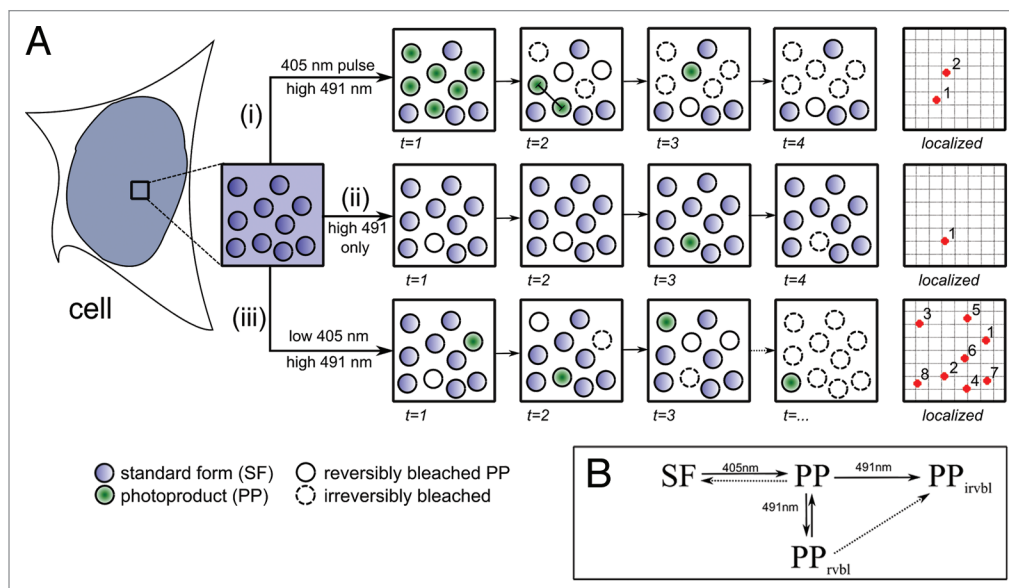
Figure 1. A putative scheme suggesting a photophysical mechanism for single molecule localization microscopy of photoconverted DNA minor groove binders, proposed on the basis of our experimental observations. Enlarged insets in (**A**) indicate DNA-bound dye molecules in a small subdiffractional area (rectangle) where only one fluorescent burst can be discerned per frame (t = 1, 2, 3, ...). Depiction of the effects of several modes of illumination: (i) High intensity 491 nm light applied after an intense 405 nm pulse: photoconverted molecules "blink" for several minutes after the pulse (in absence of the 405 nm excitation), indicating the existence of a light induced, non-emitting, reversibly bleached state; immediate saturation at the beginning of acquisition (t = 1) prevents the extraction of most single molecule signals. Closely spaced signals registered in the same frame are extracted incorrectly as a single point emitter due to diffraction (t = 2). Position coordinates are assigned to the fluorescent bursts detected in the green-yellow channel (red dots). (ii) When only high intensity 491 nm illumination is applied on the sample, blinking is rarely observed due to the low content of natively present green-emitting form of the dyes. This results in rather few localized signals in the green-yellow channel (**Fig. S1**). Spontaneous conversion of molecules to the green form might be possible; however we have no experimental proof. (iii) Simultaneous illumination of the sample with high intensity illumination at 491 nm plus low intensity illumination with 405 nm light as described in Materials and Methods. This approach allows not only an immediate registration of the blinking photoproduct after stochastic recruitment upon 405 nm illumination, but also the concomitant preservation of photophysical properties of the standard form. Time of acquisition may be freely expanded in order to register a large number of molecules in several tens of thousands of frames (t = ...). We anticipate that Hoechst and DAPI can easily be applied to localization microscopy involving sequential pulse photoconversion (405 nm) and pulse excitation (491 nm). (**B**) Proposed schemes of photoinduced reactions: SF, Standard Form; PP, green-emitting photoproduct; PP$_{rvbl}$, Reversibly bleached photoproduct; PP$_{irvbl}$, Irreversibly bleached photoproduct. The reverse reaction of photoconversion can be proposed on grounds of a chemical equilibrium. Direct transition from the reversibly bleached state to the irreversibly bleached state can, e.g., be caused by photooxidation or photolysis.

405 nm illumination the fluorescence intensity decreased to $88 \pm 5\%$ (n = 10 cells, the detailed protocol is described in Materials and Methods). A related approach, simultaneously utilizing two laser lines (for excitation and for induction of the blinking-"on"-state), was already described for other fluorophores and was named STORM[14]/dSTORM.[15] In contrast, in our protocol the two laser lines are used for generation and excitation plus reversible bleaching of the photoproduct (DAPI and Hoechst).

In order to perform single molecule localization microscopy experiments based on blinking of the green-emitting photoconverted form, the imaging buffer composition must be carefully adjusted in order to obtain a suitable blinking rate (frequency of switching between the non-emitting state and the state in which they emit fluorescent bursts, become detected and later localized). We observed a strong dependence of the blinking behavior in the green-yellow channel on the oxygen content of the embedding medium, when excited with 491 nm light (**Fig. S3**). Oxygenation was modified by an oxygen scavenging system consisting of glucose oxidase and catalase in glycerol. We then determined the optimal concentrations of these

enzymes (see Materials and Methods for details) and were able to obtain a 50-fold increase in the number of fluorescent burst signals detected, and a 200-fold increase in comparison to PBS (for detailed effects of the imaging buffer, see **Supplementary Materials** and **Fig. S3**). The optimized embedding medium was then used for all further experiments and resulted in the optical isolation and detection of numerous blinking molecules that stochastically emitted fluorescence bursts (for further information see **Fig. S3**).

We examined three bisbenzimide dyes (DAPI, and two forms of Hoechst) for use in localization microscopy of DNA with the aforementioned imaging protocol. We found that DAPI was less efficient for SMLM than Hoechst dyes, possibly due to higher crosstalk between blue-emitting and green-emitting forms which resulted in lower signal-to-noise ratio for single fluorescent molecules (**Fig. 2G**; **Fig. S2**). Thus, we favor Hoechst dyes for SMLM rather than using DAPI. Both Hoechst and DAPI exhibit a similar qualitative behavior under different illumination schemes as summarized in **Figure 1**. The use of these effects for SMLM is assessed experimentally in the following.

An application of the principle of blinking of bisbenzimide dyes is shown in **Figure 2**. It illustrates that a careful adjustment of the intensities of the 405 nm and the 491 nm lasers along with suitable imaging buffers and camera settings enabled precise localization of Hoechst 33258 molecules bound to DNA in the nucleus of a HeLa cell. All structural features of the widefield fluorescence image of the original, blue-emitting form of the dye (emission filter 470[70]) (**Fig. 2C**) are readily visible also in the localization microscopy image (**Fig. 2A**); however, the latter provides much better contrast and optical/structural resolution with much more recognizable details (**Fig. 2**, **Fig. S4**). Note that our acquisition system is optimized for SMLM measurements in terms of pixel size. Therefore, the widefield images presented as raw data are not optimal. In line with previous SPDM studies of histone H2B stably expressed with GFP,[1] the nucleus shows a pattern of higher chromatin density regions adjacent to the nuclear envelope (**Fig. 2B and F**) and around the nucleoli (**Fig. 2D**), likely representing heterochromatin. An expected lower signal density of the photoconverted form of the dye is detected in the euchromatic regions, in agreement with the wide field image.

Furthermore, we applied our photoproduct-based localization microscopy method to "nanoimaging" of mitotic chromosomes, having a higher chromatin density than in interphase. To perform highly efficient DNA localization imaging under these conditions, it was necessary not only to adjust the intensities of both laser lines (491 nm and 405 nm), but to adjust the dye concentration as well, taking into account the resulting signal density of the structure of interest. Typically, in densely labeled objects, we observed a significantly reduced precision of signal acquisition and localization due to a high fluorescence background. Hence, we used a much lower concentration of Hoechst 33342 to acquire satisfactory SMLM images of the highly condensed mitotic chromosomes. A comparison between images recorded in the conventional resolution widefield mode and in the single molecule localization mode based on the Hoechst 33342 photoproduct explicitly demonstrates that the density of DNA in a condensed chromosome is non-uniform at the nanoscale, and small regions of higher and lower DNA density can be readily recognized (**Fig. 3**). Such microdomains of different DNA densities have been anticipated in metaphase chromosomes on the basis of transmission[16] and scanning electron microscopy data,[17] as well as near-field optical microscopy.[18] Small chromatin subdomains are also predicted in chromatin coarse grain models.[19] In the case of the localization images obtained here, dense chromatin clusters are readily distinguishable in the density map in **Figure 3D**.

The mean localization accuracy in this experiment (which quantifies the precision of position estimation in localization microscopy and hence impairs the achieved optical resolution) was estimated to be approximately 14 nm using the same evaluation algorithm as in **Figure 3**, in contrast to ca. 25 nm in the case of data obtained in intact nuclei stained with Hoechst 33342. We ascribe this difference to the lower background intensities (the absence of out-of-focus contributions) and to a short distance between the imaged object and the coverslip (possibly resulting in less detectable optical aberrations originating from

differences in refractive indices). Both are due to the drastically reduced sample thickness in the case of mitotic chromosomes as compared with an interphase nucleus. However, using a different statistical noise model for the changed imaging conditions (for details see Materials and Methods), the localization precision was estimated to be 45 nm (see **Fig. 3**) (46 nm when the Thompsons' assumptions were followed[20]). Similar values for the localization precision were also obtained in localization microscopy experiments using fluorescent proteins.[21]

Discussion

It is generally accepted that nuclear chromatin is organized on several levels of compaction. While the structure of the nucleosome is well known, the higher levels of chromatin organization are a matter of continuous debate. It is also broadly believed that these structures are difficult to preserve on the nanoscale. Thus, a promising approach to study chromatin structure must include careful fixation of the whole cell rather than attempts to isolate chromatin in a native state for further studies. Electron spectroscopic imaging has opened a new avenue to localize precisely certain elements, such as phosphorus or nitrogen inside a cell nucleus.[22] However, the labeling specificity on a level of compounds, rather than elements, can be easily implemented using fluorescence microscopy. Nevertheless, until recently the optical resolution of conventional fluorescence microscopy (~200 nm in the image plane and ~600 nm axially) has been far too low to precisely study the nanostructure of chromatin. The recent progress of super-resolution optical methods such as STED, SIM, and SMLM (PALM, STORM, SPDM, GSDIM, and a number of related techniques; for review see Cremer and Masters[23]) generated the methodological basis for 3-dimensional imaging of chromatin nanostructures. The localization microscopy described in this report, based on "nanoimaging" of minor groove binding DNA dyes, constitutes the next step in this direction.

Localization microscopy of a low molecular weight fluorescent dye, which is tightly bound to DNA, offers potential advantages over the techniques that have been proposed so far. Super-resolution imaging of chromatin based on detection of the core histones is promising, but is also affected by the limited access of an antibody or detachment of histones during replication, transcription or repair. The possibility to study the DNA conformation on the nanoscale may provide key information regarding the accessibility of chromatin to these factors. Another possibility is to label the total DNA directly by means of introducing DNA precursor analogs, a technique which is expected to be limited by the toxicity of the modified nitrogen base,[8] but which could effectively be combined with our protocol. In our experiments, cells were first fixed in a way that preserves the original configuration and structure to a high degree, and then fluorescently labeled, constituting a viable option in high resolution imaging. For successful localization microscopy experiments, the fluorescence emission rate of the single molecule emitters must be high, and the blinking rate of these emitters must
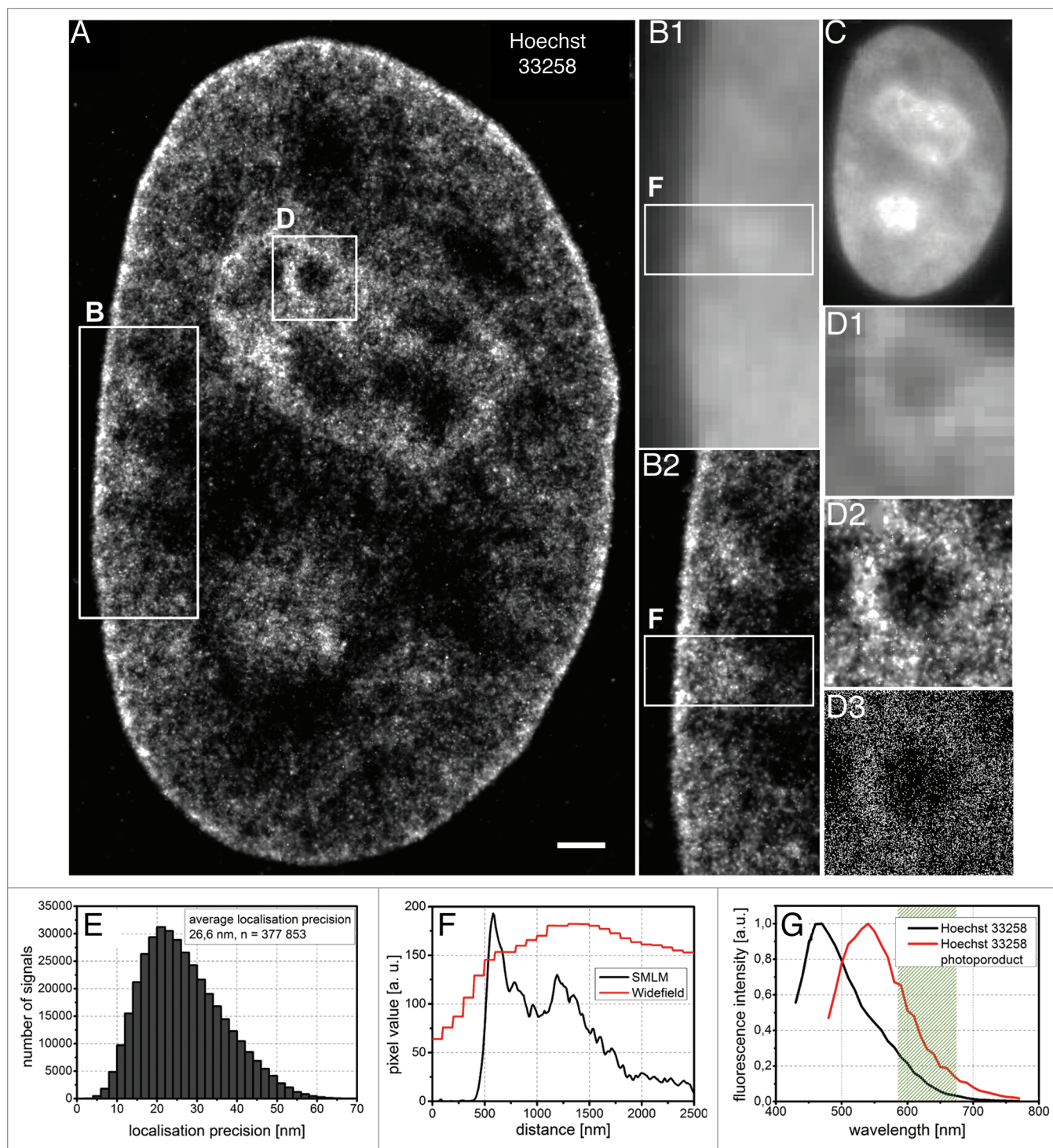
Figure 2. Structure of HeLa cell nucleus imaged by means of single molecule localization microscopy of the Hoechst 33258 photoproduct. Image acquired with high intensity laser excitation 491 nm combined with low intensity 405 nm light. (**A**) Localization microscopy of an optical plane through the entire nucleus allowed identification of approximately 400 000 signals. Localized points were blurred with the respective localization precision. Scale bar represents 1 µm. (**B**) Magnifications of a heterochromatic region in the vicinity of the nuclear envelope: (B1) widefield mode, (B2) photoproduct-based localization mode. Inserts correspond to 2.7 µm × 6.5 µm. (**C**) Raw data of a widefield preaquisition of the regular Hoechst form (λ_{exc} = 405 nm, λ_{em} = 450–490 nm). (**D**) Magnified inserts of a 1.8 µm × 1.8 µm region embracing a nucleolus: (D1) widefield mode, γ = 3, (D2) photoproduct signal positions blurred with the corresponding localization precision; (D3) point representations of localized signals. (**E**) The histogram of localization precision reveals an average value of roughly 27 nm, corresponding to an optical two-point resolution of individual molecules of about 70 nm. (**F**) Plot profile through the heterochromatic region indicated in (**B**) using widefield (red) and localization microscopy (black). (**G**) Emission spectra of DNA bound Hoechst 33258 (λ_{exc} = 405 nm, black) and its photoproduct (λ_{exc} = 458 nm, red) obtained with a confocal microscope equipped with an adjustable emission spectra (10 nm step size) as described previously.[11] The transmission band of the fluorescence emission filter used in the SMLM acquisitions is marked in green.
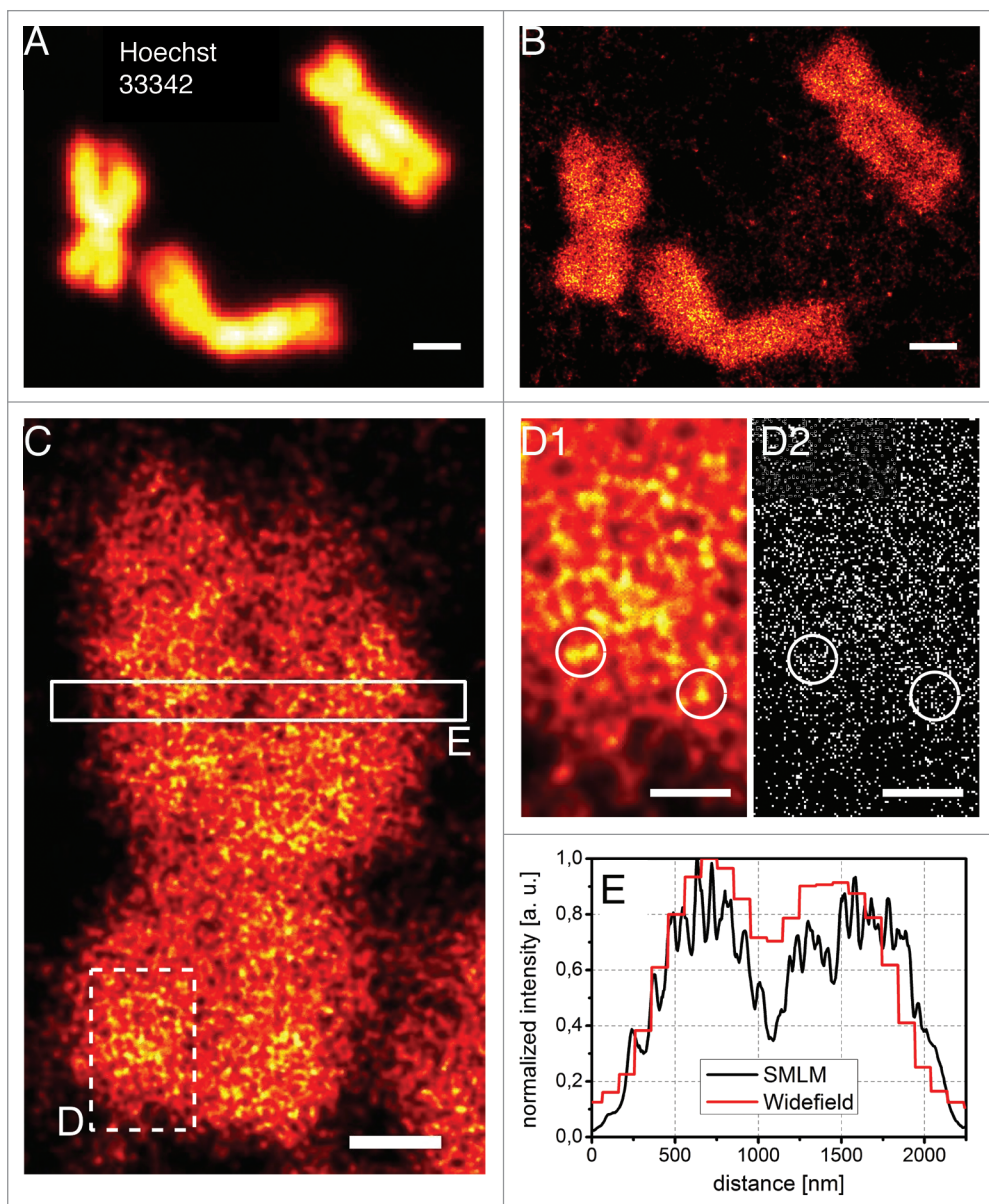
Figure 3. Single molecule localization microscopy of mitotic chromosomes stained with Hoechst 33342. Comparison of (**A**) the widefield image (raw data, collected in 450–490 nm range) and (**B**) the localization image of chromatin assessed by application of low intensity 405 nm together with high intensity 491 nm light shows the superiority of the latter. The localization image (**B**) depicts the density map of chromosomes obtained from blinking Hoechst 33342 photoproduct molecules. Common background signals stem from cellular debris containing DNA, possibly originating from detached chromatin fibers and mitochondria. Scale bar corresponds to 1 μm. (**C**) Density map assessed by means of triangulation performed on the data set acquired in the photoproduct SMLM measurement of a single chromosome. Scale bar represents 500 nm. (**E**) Plot profile through both chromatids for widefield and localization images taken from the rectangular region indicated in (**C**). Enlarged inserts indicated with the dashed line on (**C**): (**D1**) enlarged fragment of the density map, (**D2**) point representation of the data set processed for density maps, circles indicate examples of signal clusters. Scale bar in (**D**) is 200 nm. In (**E**) a spatial modulation of the signal below the diffraction limit is observed. Emission spectra of Hoechst 33342 and its photoproduct are available in **Figure S3A**.

such as bacterial chromosomes or single chromatin fibers, however with lesser success to eukaryotic nuclei.[5] The influence of intercalation between DNA bases on the overall structure of chromatin in a cell fixed by crosslinking methods is expected to be low, but needs to be investigated. Moreover, a prospect of imaging the structure of chromatin in live cells ought to be explored. It has been shown that DNA intercalators disturb interactions between the linker histone (H1) and DNA, while minor groove binders do not have such an effect.[24] Histone H1 is a key factor in the control of chromatin higher order structures. Removal of a fraction of the H1 population from the DNA results in chromatin aggregation and disturbs the nuclear structure entirely. Thus DNA intercalators do not hold promise for super-resolution imaging of DNA in live cells. In contrast, DNA minor groove binders do not interfere with the interaction between histone H1 and DNA in vivo, and do not cause chromatin aggregation and various subsequent adverse effects.[24]

As we have demonstrated in this report, three popular DNA minor groove binding dyes, Hoechst 33258, Hoechst 33342, and DAPI, can be used to reconstruct localization microscopy images of DNA by exploiting the phenomenon of their UV-induced photoconversion.[10,11] The localization microscopy images presented here depict regions of high and low DNA concentration at molecular optical resolution: on average, the smallest detectable distance between two individual Hoechst/DAPI molecules can be estimated by converting the localization accuracy to the width of the probability distribution of the position of the detected molecule (which equals ca. 2.3 times the localization accuracy achieved),[25] namely approximately 50 nm. This method of imaging cell nuclei outperforms previous conventional (**Fig. S5**)

provide for optical isolation, i.e., a sparse distribution of a few detected molecules in any acquired frame. These preconditions have been fulfilled so far by YOYO-1 and YO-PRO-1 cyanine dyes intercalating between DNA bases.[4,5] These dyes were applied to high quality localization imaging of small DNA structures

and localization-based methods in terms of resolution, sampling rate of the labeled DNA containing structure, photostability of the dyes, and simplicity of application in any laboratory without need of additional complex evaluation software as previously reported.[6] Moreover, preliminary data (not shown) suggest that combination with other SMLM compliant dyes (e.g., Alexa, Atto, etc.) is possible and in the near future shall provide a novel tool for investigations of DNA associated proteins.

In our study, we have shown that the method is capable to produce nanoscale images of the nuclear DNA distribution using standard dyes, without the need to introduce foreign genes (e.g., for GFP) or base analogs (as e.g., EdU). The single molecule localization data sets will allow a large variety of quantitative evaluations (e.g., radial density analysis[26]), as well as tests of numerical models of the mammalian genome. It may be noted that the large DNA density fluctuations (up to almost two orders of magnitude) observed on the nanoscale (see **Fig. S4**) are not in contradiction to mutually disjunct chromosome territories (potentially giving rise to a specific interchromatin compartment). Both numerical model calculations and experimental evidence indicate that such chromosome territories (except a relatively small border zone of typically a few hundred nanometers) result in nuclear zones of very low DNA density. Such zones are clearly observed in the localization images presented here. We expect that future quantitative SMLM studies will allow measurements of the extent of the interchromatin domain compartment at substantially higher resolution than conventional fluorescence microscopy.

The reconstructed images obtained by means of localization microscopy have pointillistic features, hence, discrimination of fine details depends on the density and precision of position estimation of the molecules detected.[27] A somatic cell genome consists of 6×10^9 base pairs,[28] which comprises roughly 10^8–10^9 putative binding sites for DNA minor groove binding dyes.[29] Assuming a nuclear volume of ~300 μm³ (ellipsoid with a lateral radius of 6 μm and an axial thickness of 4 μm) and an observation volume of ~50 μm³ (acquisition of the central cross-section in an optical section of ~0.5 μm thickness), approximately one sixth of these binding sites are present in the observed volume, corresponding to about 2×10^7 to 2×10^8 putative minor groove binding sites. At the present state of the art, the yield of the localization method described here allowed the identification of approximately 10^6 signals (assuming fluorescent bursts to represent individual molecules) with a concomitant loss of only 10% of fluorescence intensity after an acquisition series, which is quite difficult to achieve in localization microscopy (**Fig. S3C**). This means that even the one million of localized dye binding sites which we detected in our experiments still constitutes only a minor fraction of all the dye molecules in this region. It should be noted that the fraction of dye molecules remaining in the blue-emitting state for the entire acquisition time did not contribute to our localization images. However, it is also important to note that if one million of molecules are detected in a nuclear area of 100 μm² (and 500 nm thickness) the number of detected molecules amounts to 100×100 per 1 μm² in the image. This also means that the projected image of this slice of the nucleus contains on average one localized molecule every 10 nm in the image (the distances in 3D space are obviously larger). Therefore, it seems reasonable to state that extending the amount of data collected (i.e., recording a larger number of fluorescence bursts) will eventually enable 3-dimensional super-resolution microscopy of chromatin on the single molecule level. Thus, we anticipate that this approach holds promise for solving structure and function questions that were not accessible to optical microscopy so far. Additionally, such microscopic data will provide the basis for quantitative evaluations of the distribution of chromatin also with the help of computer models of chromatin organization.

The method can be developed further and several questions still need to be answered. These include the importance of the AT-rich sequence preference of the three dyes used here for imaging of the entire nuclear chromatin.[30,31] Studies of Hoechst 33258 in solution revealed that the fluorescence emission intensity in the presence of GC containing sequences is only half of that in the presence of AT repetitions.[30] The latter are most often involved in the formation of heterochromatin and the different emissivity presumably leads to an overestimation of heterochromatin signal density and an underestimation in euchromatic regions.

Undoubtedly, many of the photophysical effects in SMLM of DNA binding dyes are still far from understood. Developing this technology requires better comprehension of the photoconversion mechanisms and of the blinking behavior for Hoechst dyes and DAPI. Their green-emitting forms appear to be more susceptible to light-induced changes, one of which being the exploited formation of a reversibly non-emitting form (**Fig. 1**; see also **Fig. S2A**). Such a non-emitting state was already reported for many standard fluorophores such as Alexa dyes or fluorescent proteins.[1,12,32-34] One could also anticipate that, upon 405 nm illumination, the investigated dyes are converted into several chemically different forms that may interact, so cooperative effects underlying the process of blinking cannot be excluded.[35] Apart from this, the effect of the 405 nm line on the blinking behavior of the green-emitting form of the dyes needs to be investigated further (for detailed discussion see **Supplementary Materials**). In our results, multiple detection of the same fluorophore due to reoccurring blinking cannot be excluded, resulting in an overestimation of the number of molecules detected. If such multiple blinking events occur frequently for each molecule, the detected signals will form a Gaussian distribution around the center position indicating the true fluorophore position. Due to the high labeling density we could not investigate such a distribution in our experiments, however on some individual fluorophores we recognized multi-blinking behavior.

As we have shown in this report, oxygen has a major influence on the blinking characteristics of green-emitting photoproducts of DNA dyes (**Fig. S3**), and only the utilization of oxygen-depleted media may facilitate blinking rates suitable for SMLM. Interestingly, once an oxygen scavenging system is employed, blinking becomes apparent only in a narrow window of oxygen concentration. We attribute this fact to the necessity of establishing an optimal proportion between the populations of irreversibly bleached photoproduct molecules (involving oxygen[36]) and molecules moved toward some transient non-emitting state upon

high intensity 491 nm illumination (**Fig. 1**). The addition of the triplet state quencher mercaptoethylamine (MEA),[37] previously used in dSTORM switching buffers,[15] led to a nearly 40-fold loss in the number of fluorescence bursts detected (**Fig. S3**). Future photophysical studies will hopefully reveal the nature of blinking of fluorescent molecules such as the DNA-binding dyes Hoechst and DAPI.

We anticipate that the use of the DNA-minor-groove binders presented here for super-resolution localization microscopy will be of great value in furthering our knowledge about pivotal nuclear processes such as DNA replication, transcription, or repair. Moreover, the results described here are highly relevant to the contemporary challenge to acquire precise information about local DNA compaction on the single gene level (potentially in combination with fluorescence in situ hybridization, TALEN,[38] and the CRISPR/Cas system[39] as recently used in superresolution microscopy), and to obtain super-resolution spatial maps of the whole genome. So far, a major limitation in the development of super-resolution methods for imaging of DNA is the still insufficient knowledge about the photophysical and chemical mechanisms of 'blinking'. We believe that a deeper understanding herein will pave the way for true "nanoscopy" of DNA and other nuclear structures down to a few nanometers.

Materials and Methods

Cell culture and sample preparation

HeLa cervical cancer cells were grown on 0.17 mm thick coverslips in 6-well plates filled with Dulbecco's Modified Eagles Medium supplemented with 10% (v/v) fetal bovine serum in 37 °C and high humidity. After 15 min fixation with 4% formaldehyde and following permeabilization using 0.5% Triton X-100, the cells were washed with phosphate buffered saline (PBS) and treated for 1 h with a 0.5 ml solution of aqueous RNase A (0.2 mg/ml, 37 °C). Afterwards, the DNA was stained for 30 min with 1 ml aqueous solution of either Hoechst 33258 (0.2 μg/ml), Hoechst 33342 (0.1 μg/ml), or DAPI (4',6-diamidino-2-phenylindole, 0.2 μM), added directly to the 6-well plate. Such low concentrations should not provide unforeseen effects on the binding mode.[40] Subsequently, cells were washed with PBS, then embedded in a solution consisting of glycerol with 10% imaging buffer (stock comprising 0.25 mg/ml Glucose oxidase, 0.02 mg/ml Catalase, 0.05 g/ml glucose in PBS), and immediately sealed with nailpolish. Measurements were performed instantly. For chromosome spreads we performed mitotic block on HeLa cells using vinblastine (126 μM for 4 h) followed by washing with medium. Afterwards the medium with mitotic cells was collected to 14 cm³ flask and centrifuged (150 g, 5 min). Subsequently, the cell pellet was resuspended in 5 ml 75 mM KCl water solution for 10 min. Next, we added 5 ml fixative (3: 1 glacial acetic acid: methanol). After centrifugation (150 g, 5 min) cells were resuspended in ice cold fixative. This step was repeated at least 4 times. A cell suspension with 6 ng/ml Hoechst 33258 was dropped on a coverslip in horizontal position and air-dried until the fixative evaporated. Further sample preparation proceeded as mentioned above. All reagents were obtained from Sigma-Aldrich, Germany.

SPDM setup and measurements

The basic principle of the SMLM technique used here has been described in detail.[12,13] Under appropriate physicochemical conditions, the fluorophores are driven into a long-lived "reversibly bleached"/"dark" state by high intensity illumination, followed by their stochastic recovery to the fluorescent state (SPDM with physically modified fluorophores, in the following abbreviated as SPDM). Single fluorophores returning to the fluorescent state remain fluorescing only for a short period of time until they bleach permanently or return to a reversible "dark state" again. This process of switching between different absorption and/or emission states has been termed "blinking" and allows for the optical isolation and localization of single molecules with super-resolution precision (raw images available in **Fig. S2**). The calculated localization accuracy[20] (σ) is dependent on the number of detected photons (N), background noise per pixel (b), width of the point spread function (s), and pixel size (a) in the image plane and detection efficiency:

$$\sigma^2 = \frac{s^2 + a^2/12}{N} + \frac{8\pi s^4 b^2}{a^2 N^2}$$

The structural resolution in localization microscopy (R) depends on the mean localization precision of individual molecules ($< \sigma >$) and the mean distance of detected molecules, d (reflecting a quality of sampling the structure of interest):

$$R = \sqrt{(2.35 < \sigma >)^2 + (2d)^2}$$

The SPDM method as described by Lemmer et al. 2008[12] did not utilize a secondary light source for conversion or activation of fluorophores and relied solely on suitable embedding media and adjusted laser parameters (wavelength and intensity) of a single laser light source. Using suitably high illumination intensities combined with a high number of registered frames, the use of the 491 nm excitation laser alone was in principle sufficient to obtain SPDM images of the green-emitting photoproducts. For the dyes presented in this report, however, it was advantageous to also use a low intensity illumination at 405 nm in addition to high intensity illumination at 491 nm; this allowed us to increase the number of signals detected by continuously recruiting green-emitting photoproduct molecules during the measurement. Similar enhancements have been obtained in other cases also by dSTORM.[15]

For measurements, we used the custom built SMI-Vertico microscope.[13] Both spectrally distinct forms of Hoechst dyes and DAPI were illuminated with 0.002 kW/cm² by a 405 nm diode laser (Kvant Ltd) and with 1.5 kW/cm² by a 491 nm DPSS laser (Cobolt AB, Sweden). The fluorescence was detected using a 1.4 NA oil immersion objective (HCX PL APO, 63×, Leica Microsystems GmbH) and a high quantum efficiency CCD camera (SensiCam QE, PCO Imaging). To achieve the high laser intensity necessary for the localization mode, an additional achromatic lens (f = 500mm, Chroma GmbH) was used to

focus the beam. The emitted fluorescence was registered after passing through the band-pass emission filters 470(40) (Thorlabs GmbH) and 630(90) (Semrock) for the 405 nm laser and 491 nm laser, respectively. The detailed optical setup is shown in **Figure S6**.

During the experiments, raw image data stacks typically consisting of 20 000 images were recorded with an integration time of 65 ms. In these image stacks, the total number of separate fluorescent bursts identified per optical section of about 500 nm thickness through a cell nucleus ranged from about 400 000 to 2 000 000, depending on the cell line used.

To detect and localize these single bursts, we used two different algorithms written in MATLAB (The Mathworks Inc). For the images of the interphase cell nuclei we used the fastSPDM software as described by Grüll et al.[41] which is based on a center of gravity (CG) determination of the single molecule data. The software is particularly focused on high processing speed by efficient programming and possible application of field programmable gate arrays (FPGA).[41] Single molecule fluorescence bursts that were localized in several subsequent frames within the radius given by the localization accuracy were rejected by the software with only one position counted in order to avoid multiple localizations of the same fluorophore. However, a single fluorophore may emit fluorescence bursts again at later times during the measurement. Due to the stochastic nature of the fluorescent bursts, present algorithms are very limited in rejecting such temporally distant events of the same molecule; so far this constitutes an unresolved problem in the SMLM imaging method.

For the chromosome images we applied an adjusted algorithm, which uses a more complex method for the background estimation as well as a more realistic noise model and is therefore computationally more intense. Also, a more robust detection routine for closely spaced signals was included in the alternative algorithm. The localization of single events was based on CG determination of the signal weighed according to the maximum likelihood principle. A more detailed description of the algorithm is beyond the scope of this paper and shall be discussed in a subsequent publication. The raw images of the chromosomes contained, due to their condensed nature, higher local densities of blinking signals and also a strongly fluctuating background signal. The more robust alternative detection algorithm was found to be better suited for the chromosome images than fastSPDM, whereas both methods delivered very similar results for the interphase nucleus images. For reconstruction of the latter we have therefore used the previously published fastSPDM algorithm.

The long acquisition times resulted in considerable mechanical drift of the stage. We corrected the lateral drift taking advantage of the underlying structure visible in a raw image sequence (averaged over 10 subsequent frames for one sample image) and calculating the auto-correlation between sample images and fitting two (for x and y) eighth order Fourier series to the acquired data to obtain the drift vectors.

Density maps of the DNA distribution in chromosomes were obtained using a triangulation procedure. Such an approach of visualization involves iterative, multiplied reconstruction of SMLM images and was described before.[42] **Figure 3** was reconstructed using 100 iterations.

Authors' Contributions

K.P., C.C., and U.B. initiated the project. A.S., H-K.L., K.P., and D.Z-B. designed the experiments. A.S. prepared the samples and performed the single-molecule measurements. H-K.L., K.P., C.C., and U.B. developed and constructed the SPDM microscopy apparatus used in the super-resolution microscopy laboratory (Cremer-Lab) of the IMB. K.P., G.B., M.H., and U.B. contributed to the software used to data analysis. D.Z. performed the confocal experiments. K.P., A.S., H-K.L., G.B., and M.H. performed the data analysis. C.C., J.D., and U.B. supervised the work. All authors contributed in writing of the manuscript.

Supplemental Materials

Supplemental materials may be found here:
www.landesbioscience.com/journals/nucleus/article/29564

References

1. Markaki Y, Gunkel M, Schermelleh L, Beichmanis S, Neumann J, Heidemann M, Leonhardt H, Eick D, Cremer C, Cremer T. Functional nuclear organization of transcription and DNA replication: a topographical marriage between chromatin domains and the interchromatin compartment. Cold Spring Harb Symp Quant Biol 2010; 75:475-92; PMID:21467142; http://dx.doi.org/10.1101/sqb.2010.75.042

2. Matsuda A, Shao L, Boulanger J, Kervrann C, Carlton PM, Kner P, Agard D, Sedat JW. Condensed mitotic chromosome structure at nanometer resolution using PALM and EGFP- histones. PLoS One 2010; 5:e12768; PMID:20856676; http://dx.doi.org/10.1371/journal.pone.0012768

3. Cremer C, Kaufmann R, Gunkel M, Pres S, Weiland Y, Müller P, Ruckelshausen T, Lemmer P, Geiger F, Degenhard S, et al. Superresolution imaging of biological nanostructures by spectral precision distance microscopy. Biotechnol J 2011; 6:1037-51; PMID:21910256; http://dx.doi.org/10.1002/biot.201100031

4. Flors C. DNA and chromatin imaging with super-resolution fluorescence microscopy based on single-molecule localization. Biopolymers 2011; 95:290-7; PMID:21184489; http://dx.doi.org/10.1002/bip.21574

5. Schoen I, Ries J, Klotzsch E, Ewers H, Vogel V. Binding-activated localization microscopy of DNA structures. Nano Lett 2011; 11:4008-11; PMID:21838238; http://dx.doi.org/10.1021/nl2025954

6. Simonson PD, Rothenberg E, Selvin PR. Single-molecule-based super-resolution images in the presence of multiple fluorophores. Nano Lett 2011; 11:5090-6; PMID:22003850; http://dx.doi.org/10.1021/nl203560r

7. Zessin PJM, Finan K, Heilemann M. Super-resolution fluorescence imaging of chromosomal DNA. J Struct Biol 2012; 177:344-8; PMID:22226957; http://dx.doi.org/10.1016/j.jsb.2011.12.015

8. Zhao H, Halicka HD, Li J, Biela E, Berniak K, Dobrucki J, Darzynkiewicz Z. DNA damage signaling, impairment of cell cycle progression, and apoptosis triggered by 5-ethynyl-2′-deoxyuridine incorporated into DNA. Cytometry A 2013; 83:979-88; PMID:24115313; http://dx.doi.org/10.1002/cyto.a.22396

9. Rouquette J, Cremer C, Cremer T, Fakan S. Functional nuclear architecture studied by microscopy: present and future. Int Rev Cell Mol Biol 2010; 282:1-90; PMID:20630466; http://dx.doi.org/10.1016/S1937-6448(10)82001-5

10. Piterburg M, Panet H, Weiss A. Photoconversion of DAPI following UV or violet excitation can cause DAPI to fluoresce with blue or cyan excitation. J Microsc 2012; 246:89-95; PMID:22288651; http://dx.doi.org/10.1111/j.1365-2818.2011.03591.x

11. Zurek-Biesiada D, Kedracka-Krok S, Dobrucki JW. UV-activated conversion of Hoechst 33258, DAPI, and Vybrant DyeCycle fluorescent dyes into blue-excited, green-emitting protonated forms. Cytometry A 2013; 83:441-51; PMID:23418106; http://dx.doi.org/10.1002/cyto.a.22260

12. Lemmer P, Gunkel M, Baddeley D, Kaufmann R, Urich A, Weiland Y, Reymann J, Müller P, Hausmann M, Cremer C. SPDM: light microscopy with single-molecule resolution at the nanoscale. Appl Phys B 2008; 93:1-12; http://dx.doi.org/10.1007/s00340-008-3152-x

13. Reymann J, Baddeley D, Gunkel M, Lemmer P, Stadter W, Jegou T, Rippe K, Cremer C, Birk U. High-precision structural analysis of subnuclear complexes in fixed and live cells via spatially modulated illumination (SMI) microscopy. Chromosome Res 2008; 16:367-82; PMID:18461478; http://dx.doi.org/10.1007/s10577-008-1238-2

14. Rust MJ, Bates M, Zhuang X. Sub-diffraction-limit imaging by stochastic optical reconstruction microscopy (STORM). Nat Methods 2006; 3:793-5; PMID:16896339; http://dx.doi.org/10.1038/nmeth929

15. Heilemann M, van de Linde S, Schüttpelz M, Kasper R, Seefeldt B, Mukherjee A, Tinnefeld P, Sauer M. Subdiffraction-resolution fluorescence imaging with conventional fluorescent probes. Angew Chem Int Ed Engl 2008; 47:6172-6; PMID:18646237; http://dx.doi.org/10.1002/anie.200802376

16. Adolph KW, Kreisman LR, Kuehn RL. Assembly of chromatin fibers into metaphase chromosomes analyzed by transmission electron microscopy and scanning electron microscopy. Biophys J 1986; 49:221-31; PMID:3955172; http://dx.doi.org/10.1016/S0006-3495(86)83636-0

17. Harrison CJ, Jack EM, Allen TD, Harris R. Investigation of human chromosome polymorphisms by scanning electron microscopy. J Med Genet 1985; 22:16-23; PMID:4039005; http://dx.doi.org/10.1136/jmg.22.1.16

18. Winkler R, Perner B, Rapp A, Durm M, Cremer C, Greulich K-O, Hausmann M. Labelling quality and chromosome morphology after low temperature FISH analysed by scanning far-field and near-field optical microscopy. J Microsc 2003; 209:23-33; PMID:12535181; http://dx.doi.org/10.1046/j.1365-2818.2003.01101.x

19. Tark-Dame M, van Driel R, Heermann DW. Chromatin folding--from biology to polymer models and back. J Cell Sci 2011; 124:839-45; PMID:21378305; http://dx.doi.org/10.1242/jcs.077628

20. Thompson RE, Larson DR, Webb WW. Precise nanometer localization analysis for individual fluorescent probes. Biophys J 2002; 82:2775-83; PMID:11964263; http://dx.doi.org/10.1016/S0006-3495(02)75618-X

21. Gunkel M, Erdel F, Rippe K, Lemmer P, Kaufmann R, Hörmann C, Amberger R, Cremer C. Dual color localization microscopy of cellular nanostructures. Biotechnol J 2009; 4:927-38; PMID:19548231; http://dx.doi.org/10.1002/biot.200900005

22. Bazett-Jones DP, Li R, Fussner E, Nisman R, Dehghani H. Elucidating chromatin and nuclear domain architecture with electron spectroscopic imaging. Chromosome Res 2008; 16:397-412; PMID:18461480; http://dx.doi.org/10.1007/s10577-008-1237-3

23. Cremer C, Masters BR. Resolution enhancement techniques in microscopy. Eur Phys J H 2013; 38:281-344; http://dx.doi.org/10.1140/epjh/e2012-20060-1

24. Wojcik K, Dobrucki JW. Interaction of a DNA intercalator DRAQ5, and a minor groove binder SYTO17, with chromatin in live cells--influence on chromatin organization and histone-DNA interactions. Cytometry A 2008; 73:555-62; PMID:18459157; http://dx.doi.org/10.1002/cyto.a.20573

25. Kaufmann R, Lemmer P, Gunkel M, Weiland Y, Müller P, Hausmann M, Baddeley D, Amberger R, Cremer C. SPDM: single molecule superresolution of cellular nanostructures. In: Enderlein J, Gryczynski ZK, Erdmann R, editors. Proceedings of the SPIE. 2009. page 71850J–71850J–19

26. Bohn M, Diesinger P, Kaufmann R, Weiland Y, Müller P, Gunkel M, von Ketteler A, Lemmer P, Hausmann M, Heermann DW, et al. Localization microscopy reveals expression-dependent parameters of chromatin nanostructure. Biophys J 2010; 99:1358-67; PMID:20816047; http://dx.doi.org/10.1016/j.bpj.2010.05.043

27. Allen JR, Ross ST, Davidson MW. Single molecule localization microscopy for superresolution. J Opt 2013; 15:094001; http://dx.doi.org/10.1088/2040-8978/15/9/094001

28. Hattori M; International Human Genome Sequencing Consortium. Finishing the euchromatic sequence of the human genome. Nature 2004; 431:931-45; PMID:15496913; http://dx.doi.org/10.1038/nature03001

29. Loontiens FG, Regenfuss P, Zechel A, Dumortier L, Clegg RM. Binding characteristics of Hoechst 33258 with calf thymus DNA, poly[d(A-T)], and d(CCGGAATTCCGG): multiple stoichiometries and determination of tight binding with a wide spectrum of site affinities. Biochemistry 1990; 29:9029-39; PMID:1702995; http://dx.doi.org/10.1021/bi00490a021

30. Weisblum B, Haenssler E. Fluorometric properties of the bibenzimidazole derivative Hoechst 33258, a fluorescent probe specific for AT concentration in chromosomal DNA. Chromosoma 1974; 46:255-60; PMID:4136742; http://dx.doi.org/10.1007/BF00284881

31. Aymami J, Nunn CM, Neidle S. DNA minor groove recognition of a non-self-complementary AT-rich sequence by a tris-benzimidazole ligand. Nucleic Acids Res 1999; 27:2691-8; PMID:10373586; http://dx.doi.org/10.1093/nar/27.13.2691

32. Baddeley D, Jayasinghe ID, Cremer C, Cannell MB, Soeller C. Light-induced dark states of organic fluochromes enable 30 nm resolution imaging in standard media. Biophys J 2009; 96:L22-4; PMID:19167284; http://dx.doi.org/10.1016/j.bpj.2008.11.002

33. Baddeley D, Crossman D, Rossberger S, Cheyne JE, Montgomery JM, Jayasinghe ID, Cremer C, Cannell MB, Soeller C. 4D super-resolution microscopy with conventional fluorophores and single wavelength excitation in optically thick cells and tissues. PLoS One 2011; 6:e20645; PMID:21655189; http://dx.doi.org/10.1371/journal.pone.0020645

34. Huber O, Brunner A, Maier P, Kaufmann R, Couraud PO, Cremer C, Fricker G. Localization microscopy (SPDM) reveals clustered formations of P-glycoprotein in a human blood-brain barrier model. PLoS One 2012; 7:e44776; PMID:22984556; http://dx.doi.org/10.1371/journal.pone.0044776

35. Zurek-Biesiada D., Waligórski P. DJ. Mass spectrometry and fluorimetry analysis of blue-excited green-emitting protonated forms of Hoechst 33258 generated by exposure to ultraviolet light (submitted). 2014

36. Bernas T, Zarebski M, Dobrucki JW, Cook PR. Minimizing photobleaching during confocal microscopy of fluorescent probes bound to chromatin: role of anoxia and photon flux. J Microsc 2004; 215:281-96; PMID:15312193; http://dx.doi.org/10.1111/j.0022-2720.2004.01377.x

37. Song L, Varma CA, Verhoeven JW, Tanke HJ. Influence of the triplet excited state on the photobleaching kinetics of fluorescein in microscopy. Biophys J 1996; 70:2959-68; PMID:8744334; http://dx.doi.org/10.1016/S0006-3495(96)79866-1

38. Boch J, Scholze H, Schornack S, Landgraf A, Hahn S, Kay S, Lahaye T, Nickstadt A, Bonas U. Breaking the code of DNA binding specificity of TAL-type III effectors. Science 2009; 326:1509-12; PMID:19933107; http://dx.doi.org/10.1126/science.1178811

39. Anton T, Bultmann S, Leonhardt H, Markaki Y. Visualization of specific DNA sequences in living mouse embryonic stem cells with a programmable fluorescent CRISPR/Cas system. Nucleus 2014; 5:163-72; PMID:24637835; http://dx.doi.org/10.4161/nucl.28488

40. Adhikary A, Buschmann V, Müller C, Sauer M. Ensemble and single-molecule fluorescence spectroscopic study of the binding modes of the bis-benzimidazole derivative Hoechst 33258 with DNA. Nucleic Acids Res 2003; 31:2178-86; PMID:12682368; http://dx.doi.org/10.1093/nar/gkg308

41. Gruell F, Kirchgessner M, Kaufmann R, Hausmann M, Kebschull U. Accelerating Image Analysis for Localization Microscopy with FPGAs. In: 2011 21st International Conference on Field Programmable Logic and Applications. IEEE; 2011. page 1–5

42. Baddeley D, Cannell MB, Soeller C. Visualization of localization microscopy data. Microsc Microanal 2010; 16:64-72; PMID:20082730; http://dx.doi.org/10.1017/S143192760999122X